

# Dielectric and optical properties of Zr silicate thin films grown on Si(100) by atomic layer deposition

Dahlang Tahir,<sup>1,a)</sup> Eun Kyoung Lee,<sup>1</sup> Suhk Kun Oh,<sup>1</sup> Hee Jae Kang,<sup>1,b)</sup> Sung Heo,<sup>2</sup> Jae Gwan Chung,<sup>2</sup> Jae Cheol Lee,<sup>2</sup> and Sven Tougaard<sup>3</sup>

<sup>1</sup>Department of Physics, Chungbuk National University, Cheongju 361-763, South Korea

<sup>2</sup>Analytical Engineering Center, Samsung Advanced Institute of Technology, Suwon 440-600, South Korea

<sup>3</sup>Department of Physics and Chemistry, University of Southern Denmark, DK-5230 Odense M, Denmark

(Received 12 June 2009; accepted 19 September 2009; published online 29 October 2009)

Dielectric and optical properties of  $(\text{ZrO}_2)_x(\text{SiO}_2)_{1-x}$  dielectric thin films, grown on Si(100) by the atomic layer deposition method, were studied by means of reflection electron energy loss spectroscopy (REELS). The quantitative analysis of REELS spectra was carried out by using the quantitative analysis of electron energy loss spectra- $\varepsilon(k, \omega)$ -REELS software to determine the dielectric function and optical properties by using an analysis of experimental REELS cross sections from the simulated energy loss function (ELF). For  $\text{ZrO}_2$ , the ELF shows peaks in the vicinity of 10, 15, 21, 27, 35, 42, and 57 eV. For  $\text{SiO}_2$ , a broad peak at 23 eV with a very weak shoulder at 15 eV and a shoulder at 34 eV were observed, while for Zr silicates ( $x=0.75$  and  $0.5$ ), the peak position is similar to that of  $\text{ZrO}_2$ . For Zr silicates with high  $\text{SiO}_2$  concentration ( $x=0.25$ ), the peak positions are similar to that of  $\text{SiO}_2$ , but the peak at 42 eV, which is due to excitation of Zr  $N_{2,3}$  shell electrons, still exist. This indicates that the dielectric and optical properties of  $\text{ZrO}_2$  thin films are dominating the dielectric and optical properties of Zr silicates even for high  $\text{SiO}_2$  concentrations. In addition, the inelastic mean free path (IMFP) was also calculated from the theoretical inelastic cross section. The IMFP of Zr silicates increases with increasing Zr composition in Zr silicates, and they also increase with increasing primary energy. The method of determining the dielectric and optical properties and IMFP from the ELF turns out to be a convenient tool for ultrathin high- $k$  materials. © 2009 American Institute of Physics. [doi:10.1063/1.3246612]

## I. INTRODUCTION

Silicon dioxide ( $\text{SiO}_2$ ) has been used as a gate oxide in complementary metal-oxide semiconductor (CMOS) because of its stable  $\text{SiO}_2/\text{Si}$  interface as well as electrical insulation property. Recently, the rapid shrinkage of transistor feature size has forced the equivalent thickness of gate oxides to be reduced to subnanometer size in CMOS devices.  $\text{SiO}_2$  as a gate oxide material will soon face the fundamental limit due to high leakage and tunneling currents through the gate oxide. In order to avoid these physical phenomena, the gate oxide thickness should be increased by adopting high- $k$  gate dielectric materials.<sup>1</sup> The basic selection criteria for a gate oxide material are (i) large dielectric constant, (ii) a proper band offset to Si as large as or comparable to that of silicon dioxide (especially the electron injection barrier), (iii) thermodynamic stability in contact with Si substrate.<sup>2</sup> As a consequence of arduous search for materials satisfying the above criteria, transition metal oxides such as  $\text{HfO}_2$  (Refs. 2–5) and  $\text{ZrO}_2$ ,<sup>5,6</sup> and their compound with  $\text{SiO}_2$  have been proposed as the most promising high- $k$  dielectrics. In fact, the Zr based dielectrics are vigorously studied as one of the promising candidates for high- $k$  gate dielectrics. However, their dielectric and optical properties were virtually unknown. Hence, it

is worthwhile to investigate the dielectric and optical properties of Zr silicates by means of a quantitative analysis of the reflection electron energy loss spectroscopy (REELS) spectra. In our previous work,<sup>7</sup> we studied the band alignment for Zr silicates, in which we showed that the band gap, conduction band offset and valence band offset for Zr silicate thin films were similar to those of a  $\text{ZrO}_2$  thin film. At this point, we mention that REELS has been successfully used in obtaining the electronic properties of ultrathin dielectric films,<sup>5–9</sup> it provides us a straightforward way to evaluate the dielectric properties of nanodielectric thin films.<sup>10</sup> Dielectric and optical properties of nanosize gate dielectric thin films are essential to our search for good gate oxide materials in the CMOS devices. Hence, in this work, we have focused our attention to the dielectric and optical properties of nanothickness Zr silicate gate oxide thin films through quantitative analysis of REELS spectra.

## II. EXPERIMENT

$\text{ZrO}_2$  and  $(\text{ZrO}_2)_{1-x}(\text{SiO}_2)_x$  thin films were grown on  $p$ -Si (100) substrate by atomic layer deposition method. Prior to growing mixed oxide films,  $p$ -type Si substrates were cleaned by using the Radio Corporation of America (RCA) method.<sup>11</sup>  $\text{Zr}[\text{N}(\text{CH}_3)(\text{CH}_2\text{CH}_3)]_4$  and  $\text{SiH}[\text{N}(\text{CH}_3)_2]_3$  were used as precursors for  $\text{ZrO}_2$  and  $\text{SiO}_2$ , respectively, and  $\text{O}_3$  vapor served as oxygen source. The films were grown in  $\text{N}_2$  ambiance, which was supplied as the purge and carrier gas.

<sup>a)</sup>Present address: Department of Physics, Hasanuddin University, Makassar, 90245 Indonesia.

<sup>b)</sup>Author to whom correspondence should be addressed. Electronic mail: hjkang@cbu.ac.kr.

The substrate temperature was below 300 °C during the thin film deposition. The physical thickness of deposition was 7 nm. REELS spectra were obtained by using the VG ESCALAB 210 with LaB<sub>6</sub> electron gun and recorded at a constant pass energy mode of 20 eV. The incident angle of primary electrons and take-off angles of reflected electrons were 55° and 0° from the surface normal, respectively. The primary electron energies were 0.5, 1.0, 1.5, and 2.0 keV and the primary electron beam current for REELS spectrum was less than 5 nA for all energies in REELS measurement. The energy resolution, given by the full width at half maximum of the elastic peak of backscattered electrons, was about 0.8 eV, and the energy loss range was measured up to 100 eV.

### III. RESULTS AND DISCUSSION

We have studied the dielectric and optical properties of the thin films through a quantitative analysis of the electron energy-loss spectra with the Tougaard–Yubero QUEELS- $\varepsilon(k, \omega)$ -REELS software package.<sup>5,8,10,12–14</sup> The model used in this software takes into account the inelastic scattering of electrons as they travel through the vacuum above the surface, the surface region, and the bulk region of a solid, and it also takes into account the interference effects between these excitations.<sup>14</sup> In this model, all excitations are described by the dielectric function  $\varepsilon(k, \omega)$  of the material, which is the only input in the theoretical calculation of inelastic scattering cross section. Comparison of the theoretical inelastic scattering cross section to that from an experiment allows us to determine the dielectric function of a gate oxide thin film. The experimental cross section  $K_{\text{expt}}(\hbar\omega)$  times the corresponding inelastic mean free path (IMFP)  $\lambda$ , in the form of  $\lambda K_{\text{expt}}$ , is deduced from the measured REELS spectrum after correcting for the multiple scattering contributions by the formula of Tougaard *et al.*<sup>15</sup> The theoretical inelastic scattering cross section is then calculated from the dielectric response theory.<sup>12,14</sup> Assuming that the inelastic process follows a Poisson distribution, the single inelastic scattering cross section  $K_{\text{sc}}(E_0, \hbar\omega)$  can be evaluated from the inelastic scattering cross section averaged over all possible paths traveled by an electron that has been inelastically scattered only once. Here,  $E_0$  is the primary electron energy and  $\hbar\omega$  is the energy lost by an electron in a scattering event. In this model, the response of a material to a moving electron is described by the dielectric function  $\varepsilon(k, \omega)$ , which is conveniently described by the energy loss function (ELF)  $\text{Im}(-1/\varepsilon)$ . To evaluate the ELF, we parameterized it as a sum of Drude–Lindhard type oscillators, which is described in Refs. 12 and 16 as follows:

$$\text{Im}\left\{\frac{-1}{\varepsilon(k, \omega)}\right\} = \theta(\hbar\omega - E_g) \sum \frac{A_i \gamma_i \hbar\omega}{(\hbar^2 \omega_{0ik}^2 - \hbar^2 \omega^2)^2 + \gamma_i^2 \hbar^2 \omega^2}, \quad (1)$$

where the dispersion relation is given in the form

$$\hbar\omega_{0ik} = \hbar\omega_{0i} + \alpha_i \frac{\hbar^2 k^2}{2m}. \quad (2)$$

Here,  $A_i$ ,  $\gamma_i$ ,  $\hbar\omega_{0i}$ , and  $\alpha_i$  are the oscillator strength, damping coefficient, excitation energy, and momentum dispersion co-

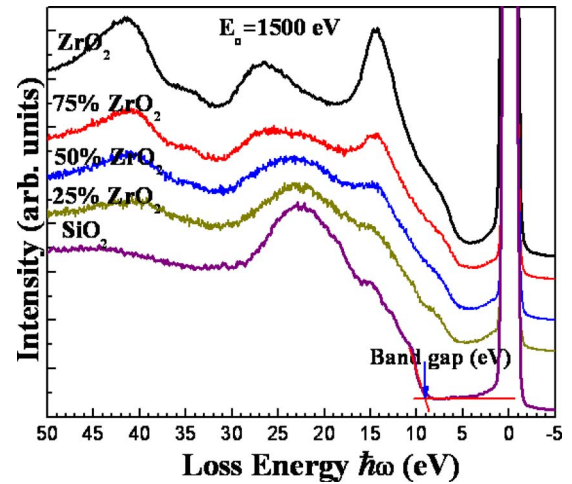


FIG. 1. (Color online) Reflection electron energy loss spectra for  $(\text{ZrO}_2)_x(\text{SiO}_2)_{1-x}$  ( $x=1, 0.75, 0.5, 0.25, 0$ ) dielectrics thin films with the primary energies of 1500 eV.

efficient of the  $i$ th oscillator, respectively, and  $\hbar k$  is the momentum transferred from the REELS electron to the solid. The dependence of  $\omega_{0ik}$  on  $k$  is generally unknown, but we can use Eq. (2) with  $\alpha_i$  as an adjustable parameter. The step function  $\theta(\hbar\omega - E_g)$  is included to describe the effect of energy band gap  $E_g$  in semiconductors and insulators. Here,  $\theta(\hbar\omega - E_g) = 0$  if  $\hbar\omega < E_g$  and  $\theta(\hbar\omega - E_g) = 1$  if  $\hbar\omega > E_g$ . The band gap was estimated from the onset value of REELS spectrum (see Fig. 1) as described in our previous paper.<sup>5,7,8</sup>

The experimental inelastic cross sections after background subtraction were fitted with fitting parameters of the  $A_i$ ,  $\gamma_i$ ,  $\hbar\omega_{0i}$ , and  $\alpha_i$ , until good agreement with the calculated inelastic cross section at several primary electron energies. The ELF  $\text{Im}(-1/\varepsilon)$  is adjusted to make sure that it fulfills the well-established Kramers–Kronig sum rule,<sup>14–16</sup>

$$\frac{2}{\pi} \int_0^\infty \text{Im}\left\{\frac{1}{\varepsilon(\hbar\omega)}\right\} \frac{d(\hbar\omega)}{\hbar\omega} = 1 - \frac{1}{n^2}. \quad (3)$$

Here,  $n$  is the index of refraction in the static limit. The indices of refraction for  $\text{ZrO}_2$  and for  $\text{SiO}_2$  are 1.8 and 1.4, respectively (see Ref. 17), and that for Zr silicates were the weighted average values for the refractive indices of  $\text{ZrO}_2$  and  $\text{SiO}_2$ . Figure 1 shows REELS spectra for  $\text{ZrO}_2$ , Zr silicate, and  $\text{SiO}_2$  dielectric thin films. The determined band gap values are 5.30, 5.35, 5.55, and 5.95 eV, respectively, for  $\text{ZrO}_2$ ,  $(\text{ZrO}_2)_{0.75}(\text{SiO}_2)_{0.25}$ ,  $(\text{ZrO}_2)_{0.5}(\text{SiO}_2)_{0.5}$ , and  $(\text{ZrO}_2)_{0.25}(\text{SiO}_2)_{0.75}$  thin films while it is 9.0 eV for  $\text{SiO}_2$ . The experimental errors of the measured band gaps are within  $\pm 0.05$  eV. In spite of the substitution of  $\text{SiO}_2$  contents in  $\text{ZrO}_2$  within this large range, band gap values of Zr silicates barely changed. Details about the band alignment of Zr silicate thin films on Si(100) can be found in Ref. 7.

Figure 2 shows the experimental  $\lambda K_{\text{expt}}$  from REELS spectra, which is compared with the theoretical  $\lambda K_{\text{sc}}$  by using the QUEELS- $\varepsilon(k, \omega)$ -REELS software. The parameters in the ELF [Eq. (1)] were determined via a trial-and-error procedure, until a satisfactory quantitative agreement is reached. Note that, in all the calculation, the same ELF was used for all energies in each composition of Zr silicates. The

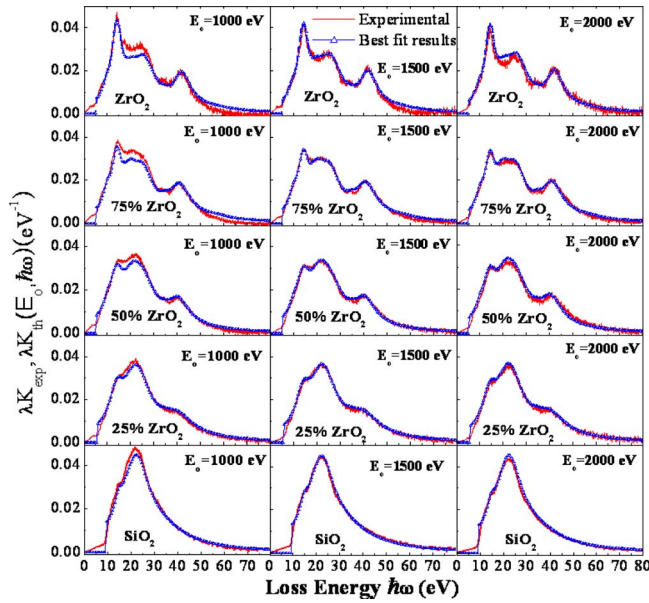


FIG. 2. (Color online) Experimental inelastic cross section  $\lambda K_{\text{exp}}$  (line), obtained from REELS data, is compared with the best fit result for the inelastic cross section  $\lambda K_{\text{sc}}$  (symbol), which is evaluated using the simulated ELF for primary energies of 1.0, 1.5, and 2.0 keV.

agreement between the theoretical results and experimental results is quite good for all energies for each material, and, hence, the experimentally observed variation in energy is well described by the theory. A small peak below the band gap ( $\sim 5$  eV) of each material, where the theory predicts no peak in this region, are due to the fact that the algorithm of Tougaard<sup>14</sup> subtracted the background from the REELS spectra using step function for the region between 0 eV and the band gap. The dielectric loss functions for Zr silicate dielectric thin films were obtained from REELS spectra for the primary electron energies of 0.5, 1.0, 1.5, and 2.0 keV.

The resulting oscillator parameters of the ELF yield the theoretical  $\lambda K_{\text{sc}}$  in good agreement with the experimental  $\lambda K_{\text{exp}}$  for all energies studied. The oscillator strengths were renormalized to fulfill the Kramers–Kronig sum rule [Eq. (3)]. The obtained parameters for the ELF of ZrO<sub>2</sub>, Zr silicate, and SiO<sub>2</sub> thin film, listed in Table I, are plotted in Fig. 3 for a wide energy range (0–80 eV). The values of the momentum dispersion coefficient  $\alpha_i$  are related to the effective mass, e.g.,  $\alpha_i \approx 0$  for insulator and  $\alpha_i \approx 1$  for metals.<sup>5,8,10</sup> In accordance with this, we found that good fits were obtained with  $\alpha_i = 0.02$  for all oscillators. The ELF  $\text{Im}(-1/\epsilon)$  and the surface ELF (SELF)  $\text{Im}[-1/(1+\epsilon)]$  for Zr silicates obtained by using these parameters are shown in Fig. 3. The ELF and SELF spectra for ZrO<sub>2</sub> and SiO<sub>2</sub> thin films are shown in Fig. 3(b). As can be seen in the figure, the intensity, the peak position, and the shape of SELF are clearly different from that of ELF.

The ELF for (ZrO<sub>2</sub>)<sub>0.75</sub>(SiO<sub>2</sub>)<sub>0.25</sub> has seven oscillators in the vicinity of 10.5, 14.8, 20.5, 26, 34.5, 41.5, and 57 eV, which are similar to those for ZrO<sub>2</sub>. The main difference is that the position of the oscillator at 42 eV is shifted to a lower energy by about 0.5 eV. For (ZrO<sub>2</sub>)<sub>0.50</sub>(SiO<sub>2</sub>)<sub>0.50</sub>, the peak positions are similar to those for (ZrO<sub>2</sub>)<sub>0.75</sub>(SiO<sub>2</sub>)<sub>0.25</sub> with the small shift in the oscillators at 20.5–21.5 eV, 41.5–

TABLE I. Parameters in the model ELFs of Zr silicates (ZrO<sub>2</sub>)<sub>x</sub>(SiO<sub>2</sub>)<sub>1-x</sub> thin films on Si (100) substrate that give the best fit overall to the experimental cross sections at 0.5, 1.0, 1.5, and 2.0 keV.

	$i$	$\hbar\omega_{0i}$ (eV)	$A_i$ (eV)	$\gamma_i$ (eV)
ZrO <sub>2</sub> ( $E_g=5.30$ ) ( $\alpha_i=0.02$ )	1	10.0	2.6	4.0
	2	15.0	44.8	3.5
	3	20.5	54.1	8.0
	4	26.5	183.8	10.0
	5	34.5	3.8	3.0
	6	42.0	215.3	8.0
	7	57.0	13.0	10.0
75% ZrO <sub>2</sub> ( $E_g=5.35$ ) ( $\alpha_i=0.02$ )	1	10.5	4.1	4.0
	2	14.8	29.0	4.0
	3	20.5	82.4	8.5
	4	26.0	133.6	9.0
	5	34.5	7.2	3.0
	6	41.5	226.2	10.0
	7	57.0	20.6	10.0
50% ZrO <sub>2</sub> ( $E_g=5.55$ ) ( $\alpha_i=0.02$ )	1	10.5	2.0	4.0
	2	14.8	30.4	5.8
	3	21.5	68.1	9.5
	4	26.0	162.9	12.0
	5	34.5	3.0	3.0
	6	40.5	161.1	10.0
	7	57.0	20.6	10.0
25% ZrO <sub>2</sub> ( $E_g=5.95$ ) ( $\alpha_i=0.02$ )	1	14.8	22.1	6.0
	2	23.5	241.3	12.5
	3	34.5	4.5	4.0
	4	40.5	171.2	15.0
SiO <sub>2</sub> ( $E_g=9.0$ ) ( $\alpha_i=0.02$ )	1	15.0	6.0	3.5
	2	23.1	225.2	11.3
	3	34.0	193.2	28.0

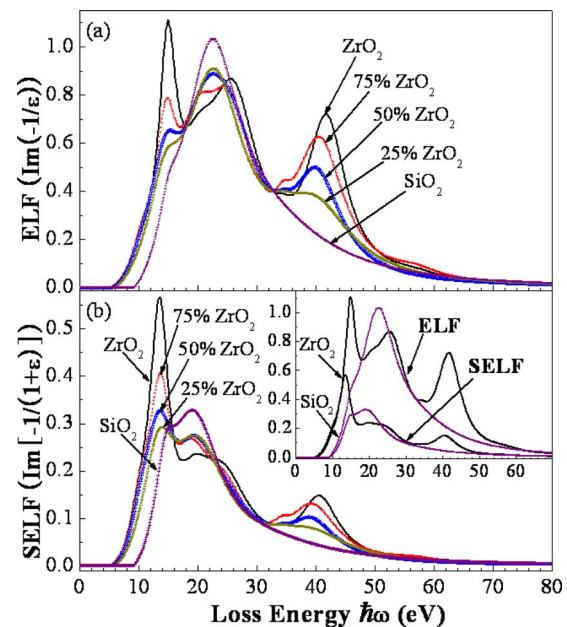


FIG. 3. (Color online) (a) ELFs and (b) SELF for Zr silicates on Si (100) substrate in this study. These ELFs are given by the parameters in Table I, which have been used as input to calculate the  $\lambda K_{\text{sc}}$  values of Fig. 2.

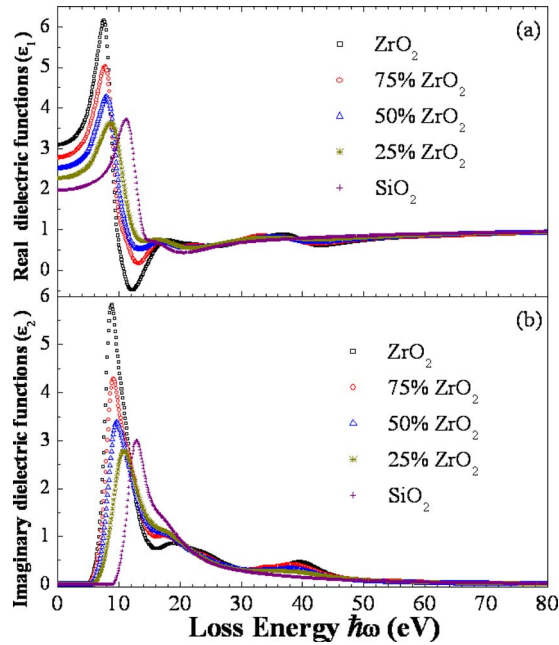


FIG. 4. (Color online) Complex dielectric function of Zr silicates on Si(100) substrate (a) Real part ( $\epsilon_1$ ) and (b) imaginary part ( $\epsilon_2$ ) of dielectric functions.

40.5 eV, and there is no oscillator at 57 eV for this composition. Intensities of the oscillators at 15 and 41.5 eV decrease with decreasing amount of Zr in silicate, while those around 18–30 eV increase with decreasing amount of Zr in the Zr silicates. For  $(\text{ZrO}_2)_{0.25}(\text{SiO}_2)_{0.75}$ , the peak positions are close to those for  $\text{SiO}_2$  as we anticipated, but the peak at 40.5 eV, which is due to  $\text{ZrO}_2$ , still exists. This result shows that the peak at 42.0 eV from  $\text{ZrO}_2$  thin film is due to the excitation of electrons from Zr  $N_{2,3}$  shell and have a strong effect on the electronic structure of Zr silicates.

We also determined the optical properties such as the index of refraction  $n$ , and the extinction coefficient  $\kappa$  from the ELF. The real part  $\text{Re}\{1/\epsilon\}$  can be obtained from the imaginary part of the ELF by making use of Kramers–Kronig relations. The real and imaginary parts of the dielectric function are as follows

$$\epsilon_1 = \frac{\text{Re}\{1/\epsilon\}}{(\text{Re}\{1/\epsilon\})^2 + (\text{Im}\{1/\epsilon\})^2}, \quad (4)$$

$$\epsilon_2 = \frac{\text{Im}\{1/\epsilon\}}{(\text{Re}\{1/\epsilon\})^2 + (\text{Im}\{1/\epsilon\})^2}.$$

The index of refraction  $n$  and the extinction coefficient  $\kappa$  are given in terms of the dielectric function as follows:<sup>16</sup>

$$n = \sqrt{\frac{1}{2}(\sqrt{\epsilon_1^2 + \epsilon_2^2} + \epsilon_1)}, \quad \kappa = \sqrt{\frac{1}{2}(\sqrt{\epsilon_1^2 + \epsilon_2^2} - \epsilon_1)}. \quad (5)$$

Figures 4 and 5 show the optical properties for Zr silicate dielectrics thin films, which were determined from the ELF in Fig. 3. Figure 4 shows the real part  $\epsilon_1$  and imaginary part  $\epsilon_2$  (corresponding to the absorption spectrum) of the dielectric function. The main peak for the real part of the dielectric function  $\epsilon_1$  is at 7.6 eV for  $\text{ZrO}_2$  and at 11.3 eV for  $\text{SiO}_2$  thin film, and that for the imaginary part of the dielectric function  $\epsilon_2$  is at 9 eV for  $\text{ZrO}_2$  and at 13 eV for  $\text{SiO}_2$  thin

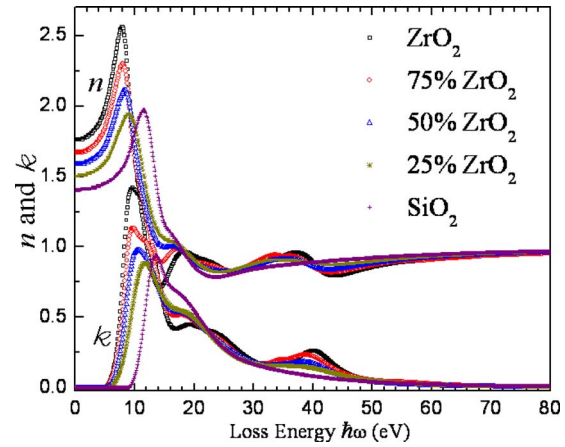


FIG. 5. (Color online) Refractive index ( $n$ ) and extinction coefficient ( $\kappa$ ) of Zr silicates on Si(100) substrate determined in this study.

film. In the absorption spectrum, which is related to  $\epsilon_2$ , the strong absorption below the main peak is associated with the transition of the valence band electrons into the unoccupied  $d$  states in the conduction bands.<sup>18</sup> The main peaks are shifted only 0.2–0.6 eV to higher energy loss position with decreasing amount of  $\text{ZrO}_2$  in Zr silicate compounds. This indicates that the dielectric functions are not linearly dependent on the amount of  $\text{SiO}_2$  in Zr silicate compounds. The dielectric functions for Zr silicate thin films, even when they contain 75%  $\text{SiO}_2$ , are close to that of  $\text{ZrO}_2$  thin film rather than that for  $\text{SiO}_2$  thin film.

Figure 5 shows the index of refraction and the extinction coefficient for these gate oxides. The main peaks of  $n$  and  $\kappa$  among the Zr silicate thin films are similar to those of  $\text{ZrO}_2$  thin films even though a large amount of  $\text{SiO}_2$  is incorporated into the  $\text{ZrO}_2$  thin films. There are only tiny energy shift of the peaks in  $\epsilon_1$ ,  $\epsilon_2$ ,  $n$ , and  $\kappa$  in Zr silicates compared with those of  $\text{ZrO}_2$  thin films. These results lead to the conclusion that  $\text{ZrO}_2$  have a strong effect on the dielectric and optical properties of Zr silicate dielectrics.

From the ELF, the IMFP can be obtained. This is of high

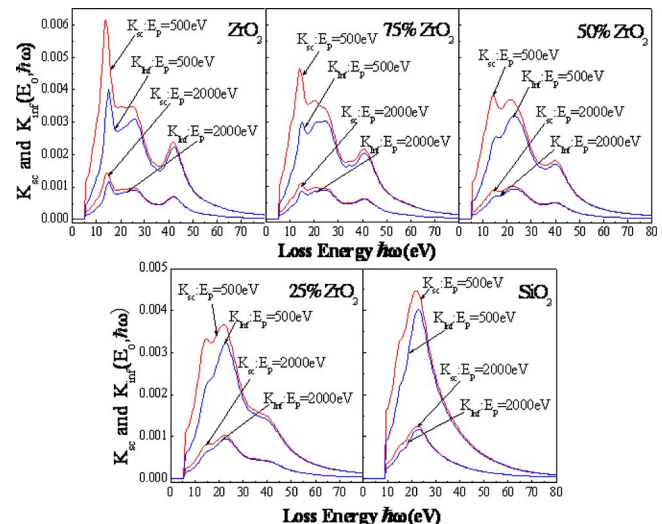


FIG. 6. (Color online) Inelastic electron scattering cross sections  $K_{sc}$ ,  $K_{inf}$  calculated with QUEELS- $\epsilon(k, \omega)$ -REELS software for Zr silicates and  $\text{SiO}_2$  thin films at the primary energies of 0.5 and 2.0 keV.

TABLE II. IMFP ( $\text{\AA}$ ) of Zr silicates for primary energies from 0.5 to 2.0 keV determined in this paper. For comparison,  $\lambda_{\text{TPP-2MM}}$  calculated from a general approximate formula (Ref. 22) are also shown.

$E_0$ (eV)	ZrO <sub>2</sub>			75% ZrO <sub>2</sub>		50% ZrO <sub>2</sub>		25% ZrO <sub>2</sub>		SiO <sub>2</sub>		
	$\lambda_{\text{TPP-2M}}$	$\lambda^{\text{sc}}$	$\lambda^{\text{inf}}$	$\lambda_{\text{TPP-2M}}$								
500	11.3	7.6	9.6	8.1	10.1	8.9	10.9	9.7	11.6	9.9	11.6	14.5
1000	18.7	14.9	17.9	15.9	18.8	17.3	20.2	18.7	21.5	18.9	21.3	24.2
1500	25.5	22.0	25.8	23.4	27.0	25.5	29.1	27.5	31.0	27.9	31.0	33.2
2000	31.9	29.0	33.4	30.8	35.5	33.6	37.8	36.2	40.2	36.6	40.0	41.8

interest because the IMFP is very important for the quantitative analysis of electron spectroscopy. Up to now, the published data on the IMFP are rather limited, and the IMFP on compound and alloy systems are rare. Figure 6 shows the comparison of the theoretical inelastic scattering cross section  $K_{\text{sc}}$  for these materials at the primary beam energy of 0.5 and 2.0 keV. Inelastic electron scattering cross section  $K_{\text{sc}}$  is defined as the probability that the electron loses energy  $\hbar\omega$  per unit energy loss and per unit path length traveled in the solid, and this includes surface, bulk, and interference excitation effects. Due to interference effects, surface excitations cannot be separated from an experimental inelastic cross section but can be calculated individually from the following expression:<sup>19–21</sup>

$$K_S = \int (K_{\text{sc}} - K_{\text{inf}}) d\hbar\omega, \quad (6)$$

where  $K_S$  is the inelastic electron scattering cross section owing to the surface,  $K_{\text{inf}}$  is the inelastic electron scattering cross section for electrons moving in an infinite medium (owing to bulk excitation). The inelastic electron scattering cross sections  $K_{\text{sc}}$  and  $K_{\text{inf}}$  calculated with the QUEELS- $\varepsilon(k, \omega)$ -REELS software for Zr silicates gate dielectrics are shown in Fig. 6. As the primary beam energy increases, the inelastic cross section generally decreases. When the primary energy becomes lower, the difference and thereby  $K_S$  becomes larger because the probability for surface excitations is higher. We also observe from Fig. 6 that, with lower primary energy, the intensities of the peaks at about 10–15 eV are enhanced relative to the peaks at about 40–50 eV, which is consistent with the SELF in Fig. 3. In this work, we determined  $\lambda^{\text{sc}}$  and  $\lambda^{\text{inf}}$  from the inverse of the theoretically determined cross section as defined in the form<sup>5,8,10,19–21</sup>

$$\lambda^{\text{sc}}(E_0) = \left[ \int_0^\infty K_{\text{sc}}(E_0, \hbar\omega) d\hbar\omega \right]^{-1}, \quad (7)$$

$$\lambda^{\text{inf}}(E_0) = \left[ \int_0^\infty K_{\text{inf}}(E_0, \hbar\omega) d\hbar\omega \right]^{-1}.$$

Here,  $\lambda^{\text{sc}}$  is the IMFP estimated from the cross section which includes both surface, bulk, and interference excitations, and  $\lambda^{\text{inf}}$  is the IMFP estimated with the cross section of the bulk excitation. These IMFP results for SiO<sub>2</sub>, Zr silicates, and ZrO<sub>2</sub> thin films with the primary electron energy of 2.0, 1.5, 1.0, and 0.5 keV are shown in Table II. The IMFP of SiO<sub>2</sub> is larger than that of ZrO<sub>2</sub>. For the Zr silicates, IMFPs increase

with decreasing Zr composition in Zr silicates, and they also increase with increasing primary energy. The IMFP values for the SiO<sub>2</sub> and ZrO<sub>2</sub> thin films estimated from the experimental inelastic scattering cross sections were compared with  $\lambda_{\text{TPP-2M}}$ , values which are calculated from the Tanuma–Powell–Penn (TPP-2M) formula.<sup>22</sup> As can be seen in Table II, the  $\lambda^{\text{sc}}$  values for ZrO<sub>2</sub> and SiO<sub>2</sub> are about 10%–20% larger than those obtained from TPP-2M, but the  $\lambda^{\text{inf}}$  values are in good agreement with those of TPP-2M. These differences between the experimentally obtained IMFP and TPP-2M IMFP could be due to surface inelastic scattering cross section which is included in the experiment value  $\lambda^{\text{sc}}$ , but it is not included in  $\lambda_{\text{TPP-2M}}$ . The IMFP estimated from the quantitative analysis of REELS provides a straightforward way to obtain the IMFP values for alloy thin films. We mention that this method was recently applied to determine the IMFP  $\lambda^{\text{sc}}$  of transition metals and ultrathin dielectric thin films.<sup>5,8,10</sup>

#### IV. CONCLUSIONS

The dielectric and optical properties of Zr silicate thin films have been obtained from a quantitative analysis of experimental REELS spectra. The dielectric functions were obtained by comparison to detailed dielectric response model calculations using the QUEELS- $\varepsilon(k, \omega)$ -REELS software package. From this, it is concluded that the  $d$  states of Zr have a strong effect on the electronic structure of Zr silicates, even when we incorporate up to 75 % SiO<sub>2</sub> into ZrO<sub>2</sub>.

The peak shapes and loss positions of ELF,  $\varepsilon_1$ ,  $\varepsilon_2$ ,  $n$ , and  $\kappa$  indicate that the ZrO<sub>2</sub> have a strong effect on the dielectric and optical properties of Zr silicate dielectric thin films. The IMFPs of the films were also determined and they increase with decreasing Zr composition in Zr silicates, and they also increase with increasing primary energy. In summary, we have demonstrated that the applied procedure for a quantitative analysis of REELS provides us with a straightforward way to determine the dielectric and optical properties and IMFP of high- $k$  thin film materials.

#### ACKNOWLEDGMENTS

This work was supported by the Korea Research Foundation Grant funded by the Korean Government (MOEHRD, Basic Research Promotion Fund) (Grant No. KRF-2008-313-C00225).

<sup>1</sup>G. D. Wilk, R. M. Wallace, and J. M. Anthony, *J. Appl. Phys.* **89**, 5243 (2001).

<sup>2</sup>M. Modreanu, J. S. Parramon, O. Durand, B. Servet, M. Stchakovsky, C.

- Eypert, C. Naudin, A. Knowles, F. Bridou, and M. F. Ravet, *Appl. Surf. Sci.* **253**, 328 (2006).
- <sup>3</sup>X. Cheng, Z. Song, J. Jiang, and Y. Yu, *Appl. Surf. Sci.* **252**, 1876 (2005).
- <sup>4</sup>R. G. Vitchev, J. J. Pireaux, T. Conard, H. Bender, J. Wolstenholme, and C. Defranoux, *Appl. Surf. Sci.* **235**, 21 (2004).
- <sup>5</sup>H. Jin, S. K. Oh, Y. J. Cho, H. J. Kang, and S. Tougaard, *J. Appl. Phys.* **102**, 053709 (2007).
- <sup>6</sup>W. J. Qi, R. Nieh, B. H. Lee, L. Kang, Y. Jeon, and J. C. Lee, *Appl. Phys. Lett.* **77**, 3269 (2000).
- <sup>7</sup>D. Tahir, E. K. Lee, S. K. Oh, T. T. Tham, H. J. Kang, H. Jin, S. Heo, J. C. Park, J. G. Chung, and J. C. Lee, *Appl. Phys. Lett.* **94**, 212902 (2009).
- <sup>8</sup>H. Jin, S. K. Oh, H. J. Kang, and S. Tougaard, *J. Appl. Phys.* **100**, 083713 (2006).
- <sup>9</sup>G. He, L. D. Zhang, G. W. Meng, G. H. Li, G. T. Fei, X. J. Wang, J. P. Zhang, M. Liu, Q. Fang, and I. W. Boyd, *J. Appl. Phys.* **104**, 104116 (2008).
- <sup>10</sup>S. Hajati, O. Romanyuk, J. Zemek, and S. Tougaard, *Phys. Rev. B* **77**, 155403 (2008).
- <sup>11</sup>W. Kern and D. A. Puotinen, *RCA Rev.* **31**, 187 (1970).
- <sup>12</sup>S. Tougaard and F. Yubero, *Surf. Interface Anal.* **36**, 824 (2004).
- <sup>13</sup>S. Tougaard and I. Chorkendorff, *Phys. Rev. B* **35**, 6570 (1987).
- <sup>14</sup>S. Tougaard and F. Yubero, QUEELS- $\varepsilon(k,\omega)$ -REELS: Software Package for Quantitative Analysis of Electron Energy Loss Spectra; Dielectric Function Determined by Reflection Electron Energy Loss Spectroscopy. Version 3.0, 2008. See (<http://www.quases.com>).
- <sup>15</sup>F. Yubero, J. M. Sanz, B. Ramskov, and S. Tougaard, *Phys. Rev. B* **53**, 9719 (1996).
- <sup>16</sup>F. Wooten, *Optical Properties of Solid* (Academic, New York, 1972).
- <sup>17</sup>[www.luxpop.com](http://www.luxpop.com).
- <sup>18</sup>L. K. Dash, N. Vast, P. Baranek, M. C. Cheynet, and L. Reining, *Phys. Rev. B* **70**, 245116 (2004).
- <sup>19</sup>N. Pauly and S. Tougaard, *Surf. Sci.* **601**, 5611 (2007).
- <sup>20</sup>N. Pauly and S. Tougaard, *Surf. Interface Anal.* **40**, 731 (2008).
- <sup>21</sup>N. Pauly and S. Tougaard, *Surf. Sci.* **602**, 1974 (2008).
- <sup>22</sup>S. Tanuma, C. J. Powell, and D. R. Penn, *Surf. Interface Anal.* **21**, 165 (1994).